

ARTICLE



Caspase-8 as a novel mediator linking Src kinase signaling to enhanced glioblastoma malignancy

Claudia Contadini^{1,2}, Alessandra Ferri^{1,2}, Marta Di Martile³, Claudia Cirotti^{1,2}, Donatella Del Bufalo³, Francesca De Nicola⁴, Matteo Pallocca⁴, Maurizio Fanciulli⁴, Francesca Sacco¹, Gloria Donninelli⁵, Alessia Capone⁵, Elisabetta Volpe⁵, Nadine Keller⁶, Shunichiro Miki⁷, Daisuke Kawauchi⁷, Dwayne Stupack⁶, Frank Furnari⁷ and Daniela Barilà^{1,2}✉

© The Author(s), under exclusive licence to ADMC Associazione Differenziamento e Morte Cellulare 2022

Caspase-8 is a cysteine protease that plays an essential role in apoptosis. Consistently with its canonical proapoptotic function, cancer cells may genetically or epigenetically downregulate its expression. Unexpectedly, Caspase-8 is often retained in cancer, suggesting the presence of alternative mechanisms that may be exploited by cancer cells to their own benefit. In this regard, we reported that Src tyrosine kinase, which is aberrantly activated in many tumors, promotes Caspase-8 phosphorylation on Tyrosine 380 (Y380) preventing its full activation. Here, we investigated the significance of Caspase-8 expression and of its phosphorylation on Y380 in glioblastoma, a brain tumor where both Caspase-8 expression and Src activity are often aberrantly upregulated. Transcriptomic analyses identified inflammatory response as a major target of Caspase-8, and in particular, NFκB signaling as one of the most affected pathways. More importantly, we could show that Src-dependent phosphorylation of Caspase-8 on Y380 drives the assembly of a multiprotein complex that triggers NFκB activation, thereby inducing the expression of inflammatory and pro-angiogenic factors. Remarkably, phosphorylation on Y380 sustains neoangiogenesis and resistance to radiotherapy. In summary, our work identifies a novel interplay between Src kinase and Caspase-8 that allows cancer cells to hijack Caspase-8 to sustain tumor growth.

Cell Death & Differentiation (2023) 30:417–428; <https://doi.org/10.1038/s41418-022-01093-x>

INTRODUCTION

Glioblastoma (GBM), the first cancer type to be systematically studied by The Cancer Genome Atlas Research Network (TCGA) [1], is the most aggressive cancer of the nervous system and is associated with a particularly poor prognosis due to its wide heterogeneity and to the lack of viable therapeutic approaches [2]. Genomic and transcriptomic analysis identified deregulation of the Receptor Tyrosine Kinases (RTKs)/Ras/Phosphoinositide 3' Kinase (PI3K) pathway as a hallmark of GBM pathogenesis [3]. Two thirds of GBM tumors exhibit aberrant activation of at least one RTK [4], that resulted in the deregulation of its downstream signaling. Src kinase represents a common hub downstream different RTKs and its aberrant activity promotes cell proliferation, migration, tumor progression, neoangiogenesis, and metastatization also in GBM [5–7]. The key role of Src in this context and the availability of FDA approved compounds targeting this kinase, prompted several studies to evaluate the significance of Src as a therapeutic target in GBM. However, clinical trials have been quite disappointing so far, stressing the necessity for studies aimed at the identification of a molecular signature for patients that may preferentially benefit from this strategy [8].

Caspase-8 is a major effector of the extrinsic apoptotic response, therefore, its expression is expected to be downregulated in cancer

[9]. An increasing quantity of gene expression data from different human tumors, however, revealed a surprising increase in Caspase-8 expression levels in many cancers, including GBM, relative to normal tissue. Interestingly, we recently reported that Caspase-8 expression positively correlates with a poorer prognosis in GBM [10], suggesting that cancer cells may switch a potential tumor suppressor into an unexpected tumor-collaborator [9–13]. Our laboratory provided the first evidence for an interplay in cancer cells between Caspase-8 and Src, showing how Src can phosphorylate Caspase-8 on Tyr380 (Y380) preventing its apoptotic activity [14, 15] and allowing Caspase-8 to modulate cell adhesion, cell migration and metastasis [16–19]. Moreover, we recently provided evidence for the aberrant phosphorylation of Caspase-8 on Y380 also in GBM cellular models [20].

Our findings raised two major questions regarding: i) the molecular pathways affected by Caspase-8 expression in GBM and ii) the molecular mechanisms that allow cancer cells to rewire its activity.

Applying a deep sequencing approach, we identify the inflammatory response and nuclear factor kappa-light-chain-enhancer of activated B cells (NFκB) signaling as the pathways preferentially affected by the downregulation of Caspase-8 expression in GBM cells. Exploring the molecular mechanism

¹Department of Biology, University of Rome "Tor Vergata", 00133 Rome, Italy. ²Laboratory of Cell Signaling, IRCCS-Fondazione Santa Lucia, 00179 Rome, Italy. ³UOSD Preclinical Models and New Therapeutic Agents Unit, IRCCS Regina Elena National Cancer Institute, Rome, Italy. ⁴UOSD SAFU, IRCCS Regina Elena National Cancer Institute, Rome, Italy. ⁵Laboratory of Molecular Neuroimmunology, IRCCS-Fondazione Santa Lucia, 00179 Rome, Italy. ⁶University of California San Diego Moores Cancer Center, La Jolla, CA 92093-0803, USA. ⁷Department of Medicine, Division of Regenerative Medicine, University of California-San Diego, La Jolla, CA 92093, USA. ✉email: daniela.barila@uniroma2.it
Edited by M. Piacentini

Received: 7 February 2022 Revised: 28 October 2022 Accepted: 11 November 2022
Published online: 2 December 2022

through which cancer cells may hijack Caspase-8 to promote NF κ B signaling and inflammation, we demonstrate that Src-dependent phosphorylation of Caspase-8 on Y380 is an important hub which sustains angiogenesis and promotes resistance to ionizing radiation. Our data identify a novel interplay between the aberrant deregulation of Src and the rewiring of Caspase-8 activity.

RESULTS

Caspase-8 modulates gene expression in glioblastoma

Caspase-8 modulates the tumorigenicity of glioblastoma cells *in vitro* and *in vivo* [10, 20]. To determine how Caspase-8 expression may impinge on gene expression in glioblastoma, we applied an unbiased comparative transcriptomic analysis of U87MG GBM cells stably silenced for Caspase-8 (shC8#1) expression or not (shCTR, scramble). This analysis identified about 23,000 genes (Table S1), among which about 14,000 quantified in shCTR or shC8#1 cells (FPKM > 0.1).

Biological replicates were highly reproducible, as shown by the high Pearson Correlation value (PC = 0.9) (Supplementary Fig. S1A). Principal component analysis revealed segregation of shCTR (sc_u87) from shC8#1 samples (shC8_u87) according to their transcriptome profile (Fig. 1A). Notably, Gene Ontology (GO) biological process enrichment analysis of the loadings driving the Principal Component Analysis (PCA) identified inflammatory response to be significantly downregulated by Caspase-8 interference (Fig. 1B).

Next, we used the DEseq2 tool to identify significantly modulated genes (FDR < 0.06 and absolute Log₂ Fold Change > 0.5). This strategy enabled the identification of 1052 genes: 527 upregulated and 525 downregulated (Table S2). To characterize biological processes and pathways that were globally and significantly enriched in our dataset, we used the DAVID functional annotation tool [21]. Genes involved in regulation of signal transduction were significantly altered by Caspase-8 interference (Fig. 1C). Again, the inflammatory response biological process was found to be significantly downregulated by Caspase-8 interference at the molecular level, suggesting that Caspase-8 might control key transcription factors which drive the inflammatory response.

To evaluate this, we next looked for transcription factors significantly enriched in our altered genes. Using the TRANSFAC dataset [22], we found that NF κ B and its subunit NF κ B p65 (also known as RelA) were among the most significantly enriched transcription factors (Table S3); indeed, most of the NF κ B targets were significantly downregulated in shC8#1 cells (Fig. 1D). qPCR analyses validated the differential expression of selected genes including NF κ B target genes identified by RNAseq (Supplementary Fig. S1B).

In parallel studies, we used the R2 Genomics Platform to identify all those genes significantly correlated with Caspase-8 expression in TCGA glioblastoma dataset (TCGA-540-MA5.0-u133a). We obtained a list of 178 genes significantly and positively correlated with Caspase-8 ($R > 0.5$, FDR < 0.05) (Table S4). In agreement with our unbiased screen data, KEGG pathway enrichment analysis of this dataset again revealed the NF κ B pathway as significantly correlated with *CASP8* (Fig. 1E). Using the TRANSFAC database, we found that genes correlating with *CASP8* were again enriched for the NF κ B and NF κ B p65 transcription factor signaling (Fig. 1E) (FDR < 0.08).

Caspase-8 expression modulates NF κ B independently of its enzymatic activity

We previously demonstrated a reduction of NF κ B signaling after Caspase-8 interference in U87MG and U251 cells [10]. This evidence was confirmed by the transcriptomic analysis described above. In addition, we evaluated this aspect in well-characterized

mesenchymal GBM patient cellular model, GBMSC83 [23, 24]; again we could appreciate after Caspase-8 silencing the reduction of NF κ B p65 phosphorylation at Serine 536 (S536), a well-known reporter of NF κ B p65 activation, and the downregulation of IL-6, IL-8 and IL-1 β mRNA levels, similarly to what observed in GBM cell lines (Supplementary Fig. S2A, B).

Next, focusing our attention on the molecular mechanisms by which Caspase-8 promotes NF κ B signaling, we first asked whether the proteolytic activity of Caspase-8 was required to modulate NF κ B p65 nuclear localization and transcriptional activity in U87MG, U251 cell lines, and in GBMSC83 cells. Cell treatment with a pan-caspase inhibitor (Z-VAD) did not affect NF κ B p65 subcellular localization (Fig. 2A). The same result was obtained also when cells were treated with TRAIL or Tumor necrosis factor alpha (TNF- α), to trigger Caspase-8 and NF κ B activity respectively (Supplementary Fig. S3A, B). Moreover, Z-VAD treatment did not affect NF κ B-responsive luciferase expression in U87MG and U251 cells (Supplementary Fig. 3C), suggesting that Caspase-8 activity is dispensable for the modulation of NF κ B signaling.

To confirm this aspect, we transiently transfected U87shC8#1 cells with Caspase-8-wt (C8-WT) or with Caspase-8 catalytically inactive (C8-C360A) (Fig. 2B). Transient reconstitution of C8-C360A in U87shC8#1 rescued NF κ B p65 nuclear localization and activity (Fig. 2C, D), similarly to C8-WT, confirming that Caspase-8 activity is dispensable for the modulation of NF κ B signaling. Interestingly, tumors with high Caspase-8 protein levels often display concomitant expression of FLICE-inhibitory protein (FLIP), which inhibits Caspase-8 and affects NF κ B activity [25, 26]. However, we found no evidence that Caspase-8 expression altered FLIP protein levels in U87MG or U251 cells (Supplementary Fig. S3D).

Src activity contributes to the modulation of NF κ B activity

Caspase-8 is phosphorylated by Src principally on Y380 in GBM cell lines [20]. To determine if this phosphorylation modulates NF κ B signaling, we initially evaluated whether alterations in Src kinase activity impinge on NF κ B function. GBMSC83, U87MG or U251 cells were treated with Dasatinib, a well-known ATP-competitive inhibitor of Src kinase activity. As expected, Dasatinib inhibited Caspase-8 phosphorylation on Y380 (Fig. 3A) and more interestingly it reduced NF κ B p65 phosphorylation on S536 (Fig. 3B). Indeed, Dasatinib treatment caused a reduction of NF κ B p65 nuclear localization (Fig. 3C), a decrease of its transcriptional activity (Supplementary Fig. S4A) and of the mRNA expression levels of several NF κ B-inflammatory target genes (Fig. 3D). Consistently, the overexpression of a catalytically inactive Src mutant (Src-K295R, Src-KD), reduced the transcription of the majority of NF κ B-inflammatory targets, compared to Src-WT (Supplementary Fig. S4B).

In contrast, the overexpression of constitutively active Src mutant (Src-Y527F) increased NF κ B p65 nuclear localization, as well as, its transcription activity and the mRNA expression levels of several inflammatory targets (Supplementary Fig. S4C–F). Interestingly, Caspase-8 silencing reduced the effect of Src-Y527F on NF κ B transcription activity, as shown in Supplementary Fig. S4G.

These data support the hypothesis that Src-dependent phosphorylation of Caspase-8 on Y380 may indeed play a role in the modulation of NF κ B activity.

Caspase-8 phosphorylation on Y380 promotes the assembly of a multiprotein complex that drives NF κ B activation

To focus on the Caspase-8 related biology downstream of Src, U87shC8#1 cells were transiently reconstituted for the expression of either Caspase-8-wt (C8-WT) or a mutant that prevents Y380 phosphorylation, Caspase-8-Y380F (C8-Y380F) (Fig. 4A). C8-WT, but not C8-Y380F, increased NF κ B p65 phosphorylation on S536 (Fig. 4A) and its nuclear localization (Fig. 4B). These results were also confirmed using an independent sequence to interfere

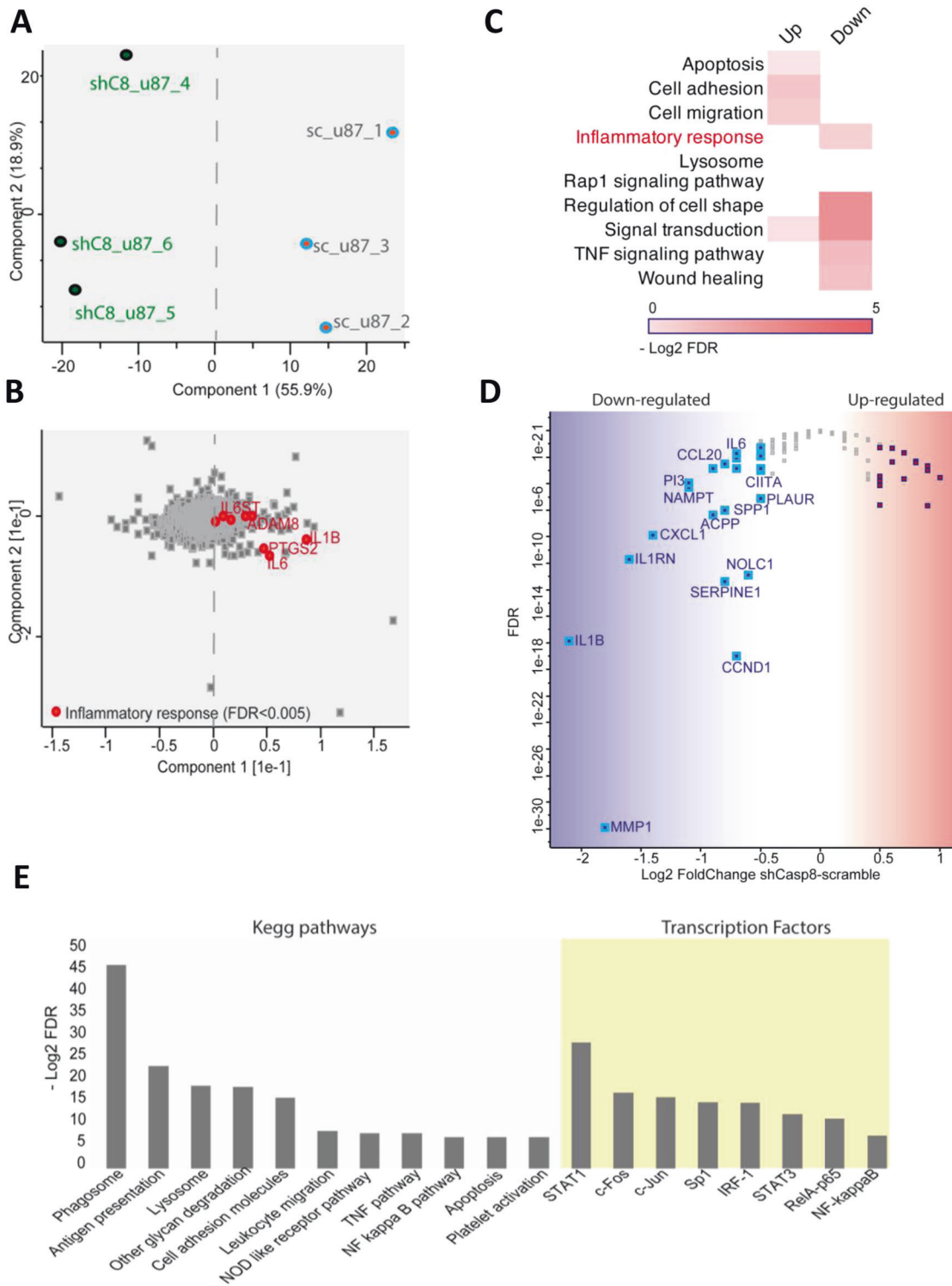


Fig. 1 Unbiased transcriptome analysis reveals Caspase-8 dependent modulation of the inflammatory response in glioblastoma. **A** Principal component analysis (PCA) of glioblastoma cell lines discriminates the control cells (sc_sample) from Caspase-8 interfered ones using the shC8#1 sequence (shC8_sample). **B** Loadings of A reveal that the transcripts responsible for driving the segregation in component 1 are significantly enriched in specific GO-biological processes (FDR < 0.05). **C** GO-Biological processes and KEGG pathways significantly enriched in downregulated and upregulated proteins are shown in the heatmap (FDR < 0.05). **D** Scatterplot of NFκB targets, as reported in the TRANSFAC database. **E** Bar graph reporting KEGG pathways and transcription factor significantly enriched in R2 Caspase-8 correlated genes.

Caspase-8 expression (shC8#2) in U87MG and in GBMSC83 cells. Again, the stable reconstitution of C8-WT but not of C8-Y380F expression promoted NFκB p65 phosphorylation at Ser536 and its nuclear localization (Supplementary Fig. S5A, B).

Interestingly, we could not detect any Caspase-8 translocation in the nucleus, as shown in both U87MG and U251 (Supplementary Fig. S6), thereby suggesting a role for Caspase-8 in the early stages of NFκB activation in the cytosol [27]. Coimmunoprecipitation

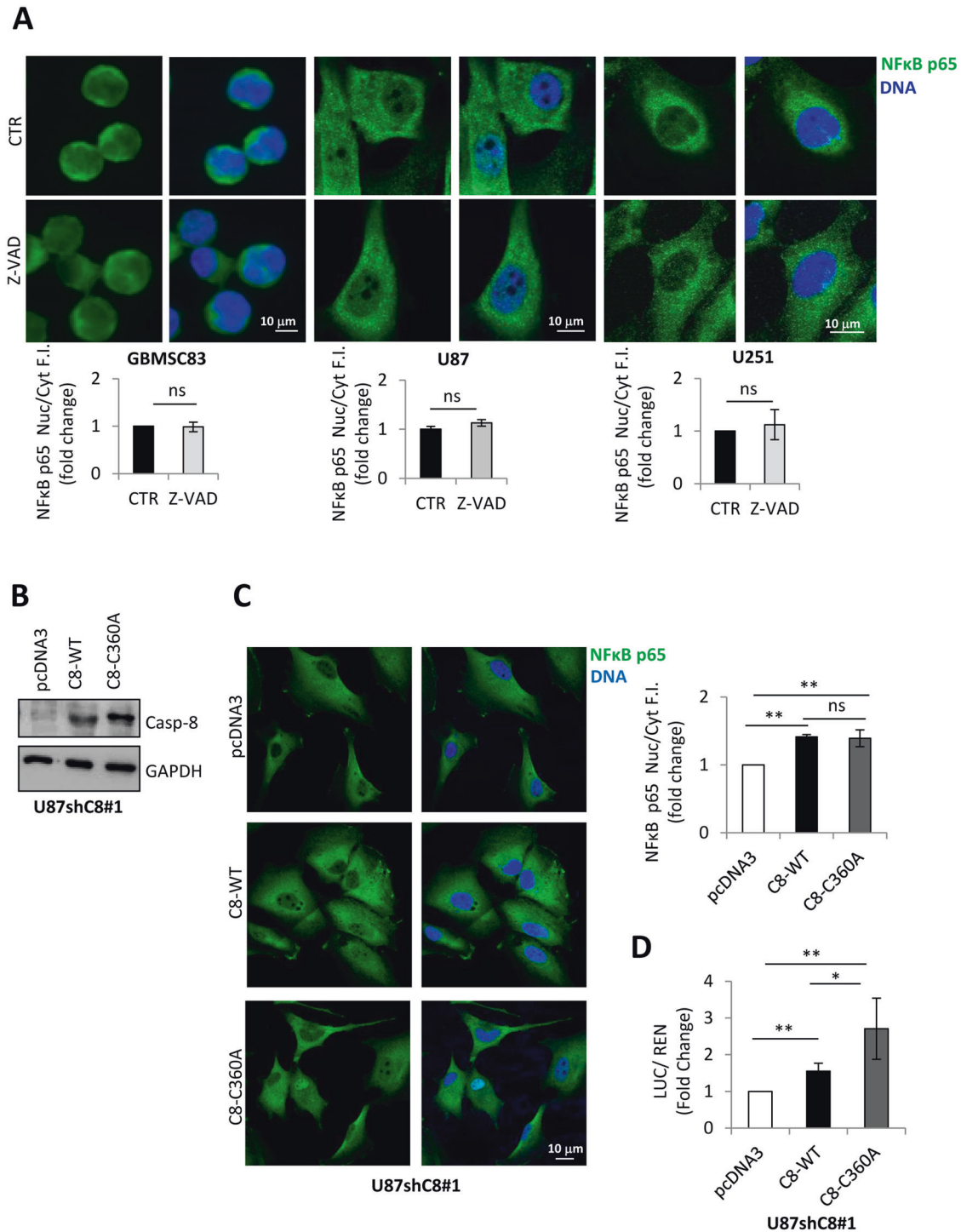


Fig. 2 Caspase-8 expression modulates NFκB independently of its enzymatic activity. **A** Immunofluorescence analysis for NFκB p65 (green) and DNA (DAPI, blue) in GBMSC83, U87MG and U251 upon Z-VAD treatment (10 μM for 24 h) compared to CTR (DMSO) cells. Bar scale: 10 μm. The bar chart represents the nuclear (NUC)/cytoplasmic (CYT) ratio of NFκB p65 staining (F.I. = fluorescence intensity). **B** Immunoblotting on total protein extracts from U87MG cells stably silenced for Caspase-8 expression (U87shC8#1) and transiently transfected with the empty vector (pcDNA3), Caspase-8-wt (C8-WT) or the catalytically inactive mutant, Caspase-8-C360A (C8-C360A). GAPDH was used as loading control for protein normalization. **C** Immunofluorescence analysis for NFκB p65 (green) and DNA (DAPI, blue) in U87shC8#1 transiently transfected as in B and processed as in A. **D** Histogram representing NFκB transcriptional activity measured by Luciferase assay on U87shC8#1 transfected as in B. Statistical analysis was performed by the unpaired Student's *t*-test (ns= not significant; **P* ≤ 0.05; ***P* ≤ 0.01). Results represent the mean of three independent experiments ± SD.

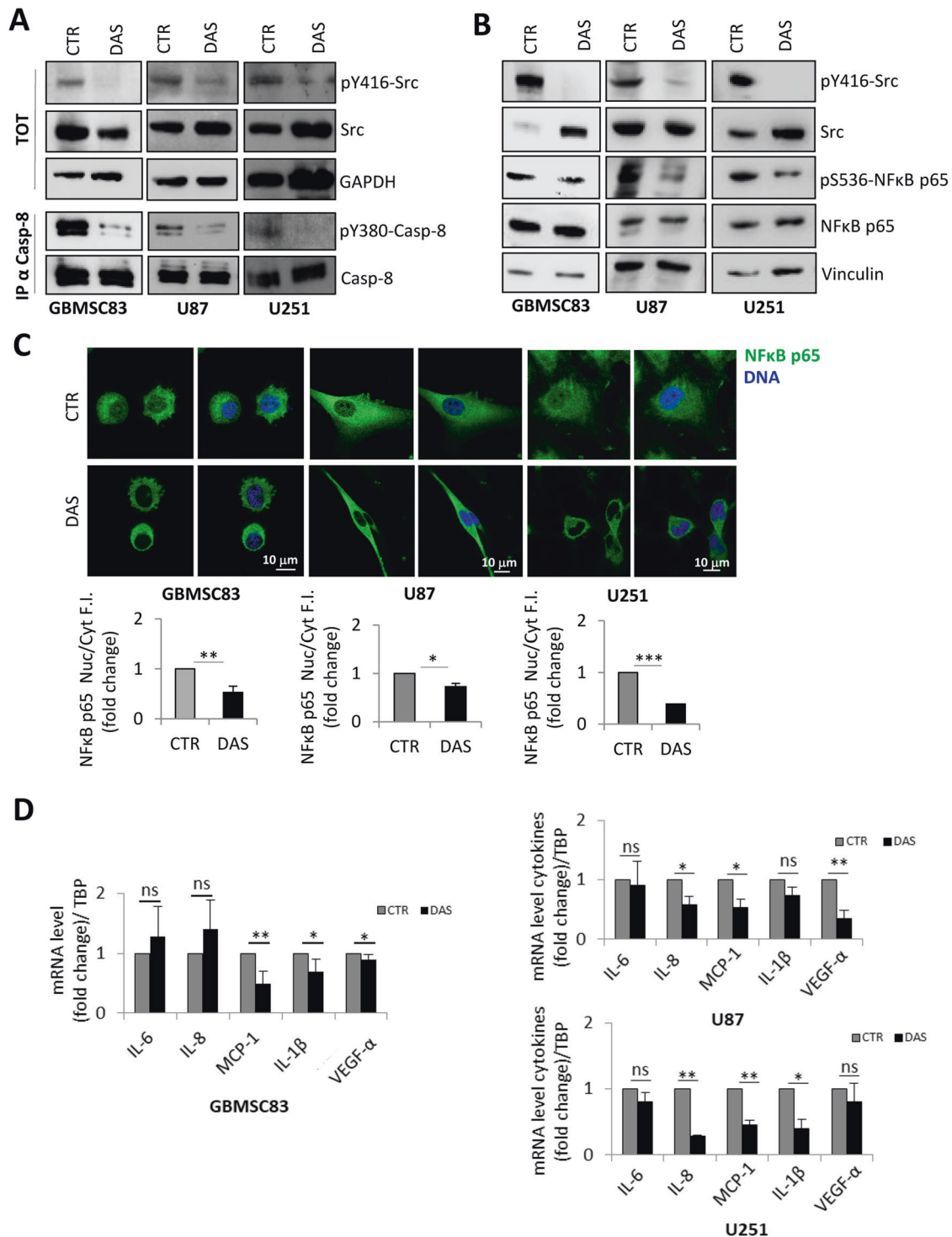


Fig. 3 Src activity sustains NFκB p65 nuclear localization and promotes its transcriptional activity. **A** Immunoblotting on total protein extracts (TOT) and on immunoprecipitated Caspase-8 (IP) from GBMSC83, U87MG and U251 cells treated with Dasatinib 1 μM (DAS) or not (DMSO, CTR) for 16 h. GAPDH and Caspase-8 were used as loading controls for protein normalization. **B** Immunoblotting on total protein extracts from GBMSC83, U87MG and U251 cells incubated or not with DAS 10 nM for 16 h. NFκB p65 phosphorylation at S536 was normalized on NFκB p65 protein total level. **C** Immunofluorescence analysis for NFκB p65 (green) and DNA (DAPI, blue) on GBMSC83, U87MG and U251 cells treated as in B. Bar scale: 10 μm. The bar chart represents the nuclear (NUC)/cytoplasmic (CYT) ratio of NFκB p65 staining. (F.I. = fluorescence intensity). **D** qPCR on GBMSC83, U87MG and U251 cells after DAS treatment compared to CTR cells. The mRNA levels of the inflammatory factors targeted by NFκB (*i.e.*, IL-6, IL-8, MCP-1, IL-1β, and VEGF-α) were normalized using TBP as housekeeping gene. Statistical analyses were performed by the unpaired Student's *t*-test (ns = not significant; **P* ≤ 0.05; ***P* ≤ 0.01; ****P* ≤ 0.001). Results represent the mean of three independent experiments ± SD.

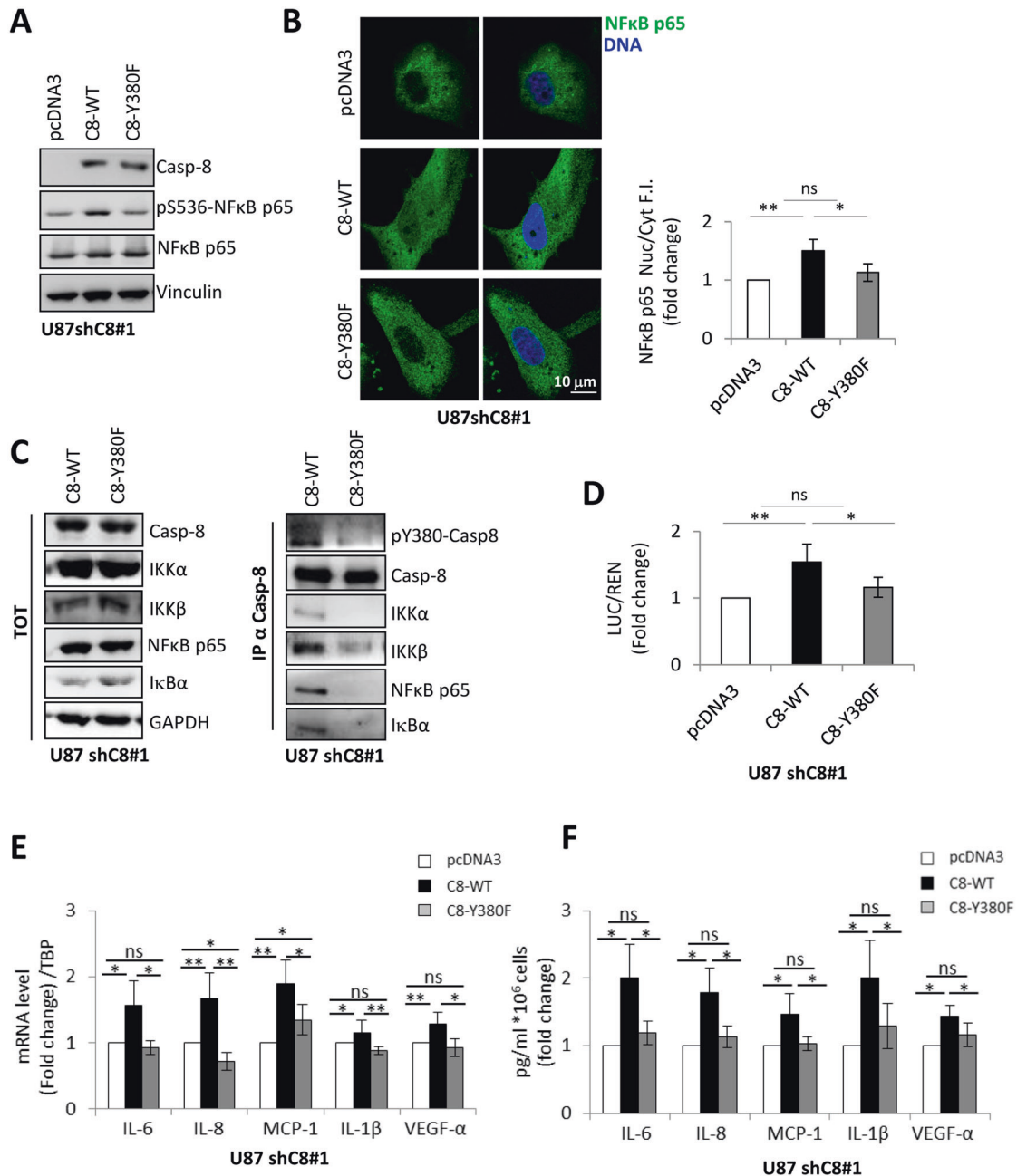


Fig. 4 Src-dependent phosphorylation of Caspase-8 on Y380 contributes to recruitment of NFκB p65 to a multiprotein complex promoting its activation. **A** Immunoblotting on total protein extracts from U87MG cells stably silenced for Caspase-8 expression (U87shC8#1) and transiently transfected with the empty vector (pcDNA3), Caspase-8-wt (C8-WT) or the unphosphorylatable mutant, Caspase-8-Y380F (C8-Y380F). Vinculin was used as loading control for protein normalization. **B** Immunofluorescence analysis for NFκB p65 (green) and DNA (DAPI, blue) in U87shC8#1 cells transfected as described in **A**. Bar scale: 10 μm. The bar chart represents the nuclear (NUC)/cytoplasmic (CYT) ratio of NFκB p65 staining. (F.I. = fluorescence intensity). **C** Immunoblotting on total protein extracts (TOT) and immunoprecipitated Caspase-8 (IP) derived from U87shC8#1 cells transiently transfected with C8-WT or C8-Y380F. **D** Histogram representing NFκB transcriptional activity measured by Luciferase assay on U87shC8#1 cells transfected as in **A**. **E** qPCR on U87shC8#1 cells transfected as in **A**. The mRNA levels of the inflammatory factors targeted by NFκB (i.e., IL-6, IL-8, MCP-1, IL-1β, and VEGF-α) were normalized using TBP as housekeeping genes. **F** Fold change of the concentrations (pg/ml) of the inflammatory factors targeted by NFκB (i.e., IL-6, IL-8, MCP-1, IL-1β, and VEGF-α) were measured by Luminex assay, in the conditioned media (CM) of U87shC8#1 cells transfected as in **A**. The volume of CM from different samples was normalized on the number of cells for each sample counted when CM was collected. Statistical analyses were performed by the unpaired Student's *t*-test (ns = not significant; **P* ≤ 0.05; ***P* ≤ 0.01; ****P* ≤ 0.001). Results represent the mean of at least three independent experiments ± SE.

experiments revealed a multiprotein complex where C8-WT is associated to NFκB p65 protein, its upstream activating kinases IKKα/β proteins and its inhibitor IκBα (Fig. 4C). Importantly, these interactions are severely reduced in cells reconstituted for the

expression of C8-Y380F mutant (Fig. 4C). In agreement with this, C8-WT, but not C8-Y380F, promoted NFκB transcriptional activity (Fig. 4D) and sustained the mRNA and protein expression of its inflammatory targets (Fig. 4E, F).

Interestingly, the expression of the phospho-mimetic Caspase-8-Y380D (C8-Y380D) in U87shC8#1 cells showed a behavior similar to C8-WT, compared to C8-Y380F (Supplementary Fig. S7A–C).

Overall, these studies support the conclusion that Src kinase-dependent phosphorylation of Y380 enables Caspase-8 to promote the activation of NF κ B and the expression of its target inflammatory genes.

Caspase-8 phosphorylation on Y380 is required for the pro-angiogenic activity of Caspase-8

We have previously shown that Caspase-8 expression in GBM cells promotes angiogenesis *in vitro* and *in vivo* [10]. To test whether Src-dependent phosphorylation on Y380 may be required for the angiogenic activity of Caspase-8, Human Umbilical Vein Endothelial Cells (HUVECs) were grown in the presence of conditioned media (CM) from U87shC8#2 cells, stably reconstituted or not for Caspase-8-wt (C8-WT) or Caspase-8-Y380F mutant (C8-Y380F). Importantly, when exposed to CM from C8-WT cells, HUVECs formed tube-like structures resembling a capillary plexus. In contrast, poorly organized and rounded endothelial cells were observed after the addition of CM from C8-Y380F (Fig. 5A, B).

To further investigate whether Y380 phosphorylation may support angiogenesis, we evaluated neovascularization *in vivo* in matrigel plugs-containing CM collected from U87shC8#2 cells or from daughter cells stably reconstituted with C8-WT or C8-Y380F. Matrigel plugs-containing CM from shC8#2 cells or those reconstituted with C8-Y380F showed a depressed angiogenic response, differently from CM from C8-WT, as revealed by macroscopic analysis and hemoglobin content quantification (Fig. 5C, D). Importantly, results from experiments performed on GBMSC83shC8#2 cells reconstituted or not with C8-WT or C8-Y380F, further supported a role for pY380 Caspase-8 in neoangiogenesis (Fig. 5E, F).

To evaluate the ability of Caspase-8 expression and of its Y380 phosphorylation to modulate tumorigenesis and neoangiogenesis *in vivo*, GBMSC83shC8#2 cells reconstituted or not with C8-WT or C8-Y380F were intracranially injected in mice. Although all GBMSC83 cells were able to induce tumor growth, a strong hemorrhagic response triggered the death of mice independently of the tumor growth. We next sought to evaluate neovascularization in tumors obtained from shC8#2, C8-WT and C8-Y380F cells. Tumor vessels were visualized using anti-CD31 mAb, which permitted an assessment of vascular density within the tumors. As shown in Fig. 5G, a significant difference in vascularization was detected between C8-WT and C8-Y380F tumors. Collectively, these results support the requirement of pY380 Caspase-8 for neoangiogenesis.

Caspase-8 phosphorylation on Y380 promotes GBM cells resistance to radiotherapy

To evaluate whether Src-Caspase-8 axis affects GBM response to radiotherapy, clonogenic and MTS assay were performed on U87shC8#2 cells stably reconstituted with C8-WT or C8-Y380F upon ionizing radiation (IR, 5 Gy or 10 Gy). Again, C8-WT but not C8-Y380F, rescued cell proliferation and viability of U87shC8#2 cells (Fig. 6A–D). Although IR significantly impaired colony formation and cell viability in all conditions, the expression of C8-WT but not C8-Y380F impinges on the efficiency of this treatment (Fig. 6A–D). Moreover, cell death after IR (10 Gy) was evaluated by flow-cytometry analysis in GBMshC8#2 reconstituted with C8-WT or C8-Y380F, confirming that C8-WT but not C8-Y380F expression protected cells from IR induced cell death (Fig. 6E, F). These studies, together, provide compelling evidence that impairing Caspase-8 phosphorylation on Y380 may enhance GBM sensitivity to IR.

DISCUSSION

GBM is a very aggressive tumor with a 5-year survival rate of less than 5% [2]. Genomic and transcriptomic analyses have been performed in order to improve glioblastoma classification on the

base of their molecular abnormalities with the final aim to achieve an efficient patient stratification. These studies initially classified GBM into 4 major subtypes: Proneural, Neural, Classical, and Mesenchymal each characterized by specific abnormalities [3]. The mesenchymal subtype, mainly characterized by aberrantly low expression of NF1 and PTEN, displays also significantly higher levels of Caspase-8, supporting the idea that some tumors may rewire Caspase-8 activity from apoptosis to alternative functions that overall may support tumor progression and therapy resistance [3]. We previously provided evidence for such a role in GBM cells, showing that Caspase-8 promotes tumorigenicity and supports the activation of NF κ B which in turn triggers the expression of some inflammatory factors [10].

Our transcriptomic analysis on a GBM cellular model supported a significant downregulation of the inflammatory response and of NF κ B signaling upon Caspase-8 suppression (Fig. 1) across several lines of analysis. This was mirrored in the clinical data provided within the TCGA GBM dataset confirming our *in vitro* experimental data (Fig. 1), suggesting a significant role for Caspase-8-NF κ B-inflammatory factors axis in GBM development and progression.

Although Caspase-8 has been previously connected to NF κ B transcriptional activity [28], this link has been largely confined to the immune system [29, 30]. Much less is known regarding the role of this interplay in tumor cells, and the rewiring of tumor cells to mimic this signaling axis represents a significant factor governing GBM malignancy. Whether Caspase-8 enzymatic activity is dispensable or not for NF κ B activation is still debated [27, 31, 32]. In our experimental system the enzymatic activity of Caspase-8 is not required to modulate NF κ B p65 subcellular localization or transcriptional activity (Fig. 2). These data support the idea that Caspase-8 may indeed act as a platform [27] to allow the assembly of the multiprotein complex that promotes NF κ B p65 phosphorylation, and thereby its subsequent activation. Indeed, the demonstration that Caspase-8 coimmunoprecipitates with IKK α / β , I κ B α and NF κ B p65 strongly supports this notion. It remains possible that Caspase-8 phosphorylation acts as a critical shunt during GBM tumorigenesis, avoiding apoptosis and activating tumor-promoting NF κ B signaling (Fig. 7).

Our laboratory first identified Caspase-8 as a Src substrate, with phosphorylation on Y380 preventing its apoptotic activity [14]. Indeed, Y380 is located in a short linker removed via the maturation cleavages required for the assembly of the fully active tetrameric complex [14]. NMR studies supported these early observations [33, 34]. The interplay between Src and Caspase-8 may significantly contribute to rewire Caspase-8 activity in cancer (reviewed in [19]). We previously documented that Caspase-8 is aberrantly phosphorylated on Y380 by Src kinase in GBM cells [20]. Here, we have defined a role of Src-dependent phosphorylation on Y380 as part of the molecular mechanism that allows Caspase-8 to promote NF κ B activity and contributes to angiogenesis. Consistently with this, we have previously shown that hypoxic conditions, which usually trigger neoangiogenesis, promote Src activity and Caspase-8 phosphorylation on Y380 [20].

In agreement with the idea that Y380 phosphorylation dampens Caspase-8 apoptotic potential, we observed that Caspase-8-wt, but not Caspase-8Y380F, confers resistance to ionizing radiation (Fig. 6), commonly used to treat GBM patients. These results suggest that the interplay between Src and Caspase-8, that leads to Y380 phosphorylation, may have a potential role also in cancer recurrence (Fig. 7) [35, 36].

Src kinase is often upregulated in many tumors including GBM [7, 8]. Genomic studies rarely detect Src mutations in tumors, however Src aberrant activation has been clearly connected to the occurrence of mutations or increased copy number of an upstream RTKs and to PTEN loss of function, that overall identify signaling nodes frequently deregulated in cancer, pointing to Src as a valuable target to improve the efficacy of radio and chemotherapy.

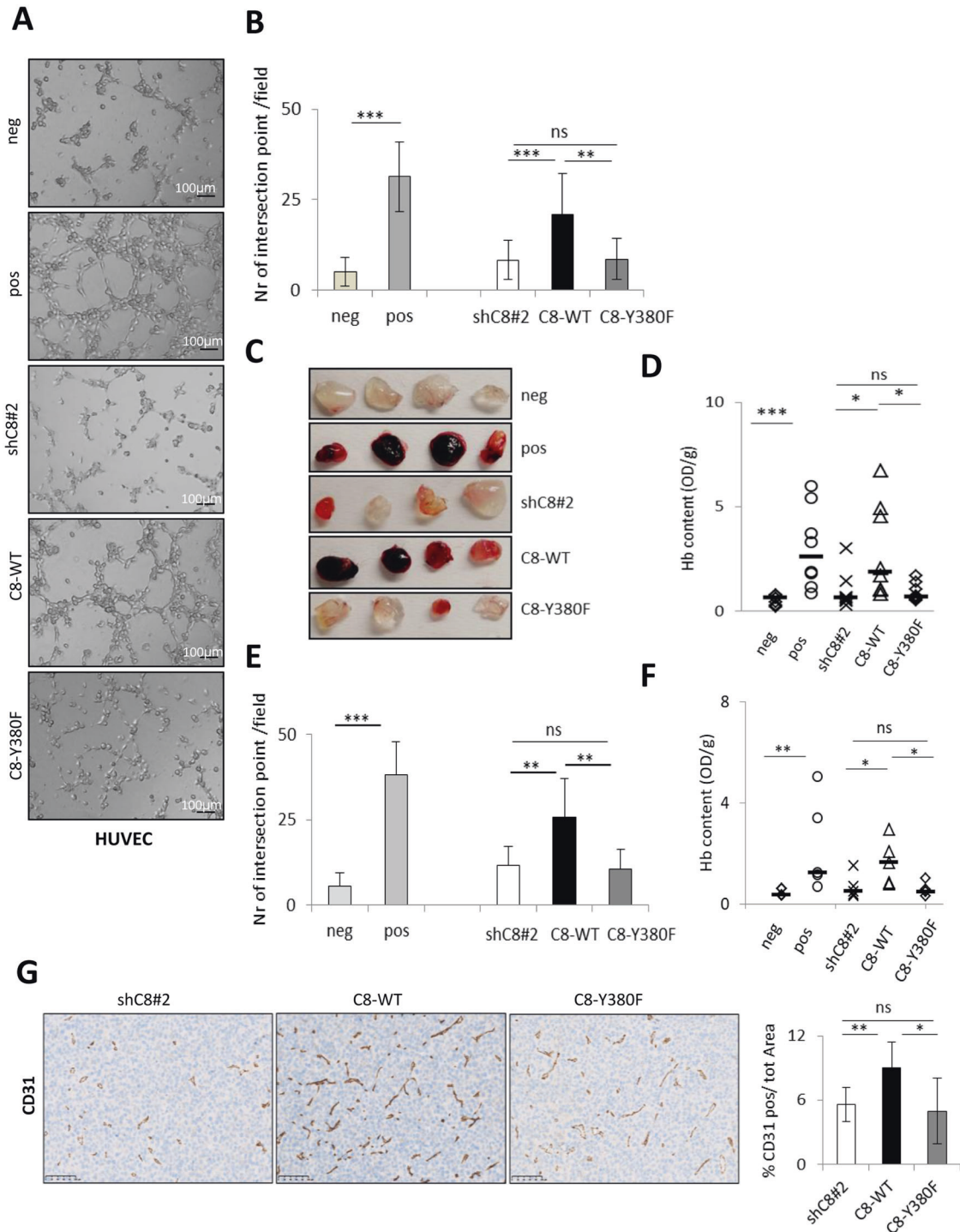


Fig. 5 Src-dependent phosphorylation of Caspase-8 on Y380 is required for the pro-angiogenesis activity of Caspase-8. Representative images (**A**) and relative quantification (**B**) of HUVEC capillary tube-like network formation on Cultrex after exposure for 6 h to Conditioned Media (CM) from U87shC8#2 cells reconstituted with pLV-EF1a IRIS vector encoding for Caspase-8-wt (C8-WT) or the unphosphorylatable mutant, Caspase-8-Y380F (C8-Y380F). Scale bar 100 μ m. Results represented the mean of number of intersection points/field \pm SD of three independent experiments. Representative images (**C**) and quantification of Hemoglobin content (**D**) of Matrigel plugs-containing CM from U87shC8#2, and shC8#2 cells reconstituted as in **A**. Plugs containing heparin alone (neg) or heparin plus VEGF (pos) were used as negative or positive control, respectively. Quantification of HUVEC capillary tube-like network formation (**E**) and Hemoglobin content of Matrigel plugs (**F**) derived from CM of GBMSC83shC8#2, and shC8#2 cells reconstituted with C8-WT or C8-Y380F as described above. The results are represented as median of each condition and were expressed as OD540nm/g of Matrigel plugs. **G** Representative images of CD31 staining in brain slices of mice injected with either GBMSC83shC8#2, GBMSC83shC8#2-C8-WT or GBMSC83shC8#2-Y380F. The histogram represents the % of CD31 positive fields over total analyzed tumor area. Original magnification $\times 20$, scale bar 100 μ m. Statistical analyses were performed by the unpaired Student's *t*-test (ns = not significant; **P* \leq 0.05; ***P* \leq 0.01). Results represent the mean of at least three independent experiments \pm SD.

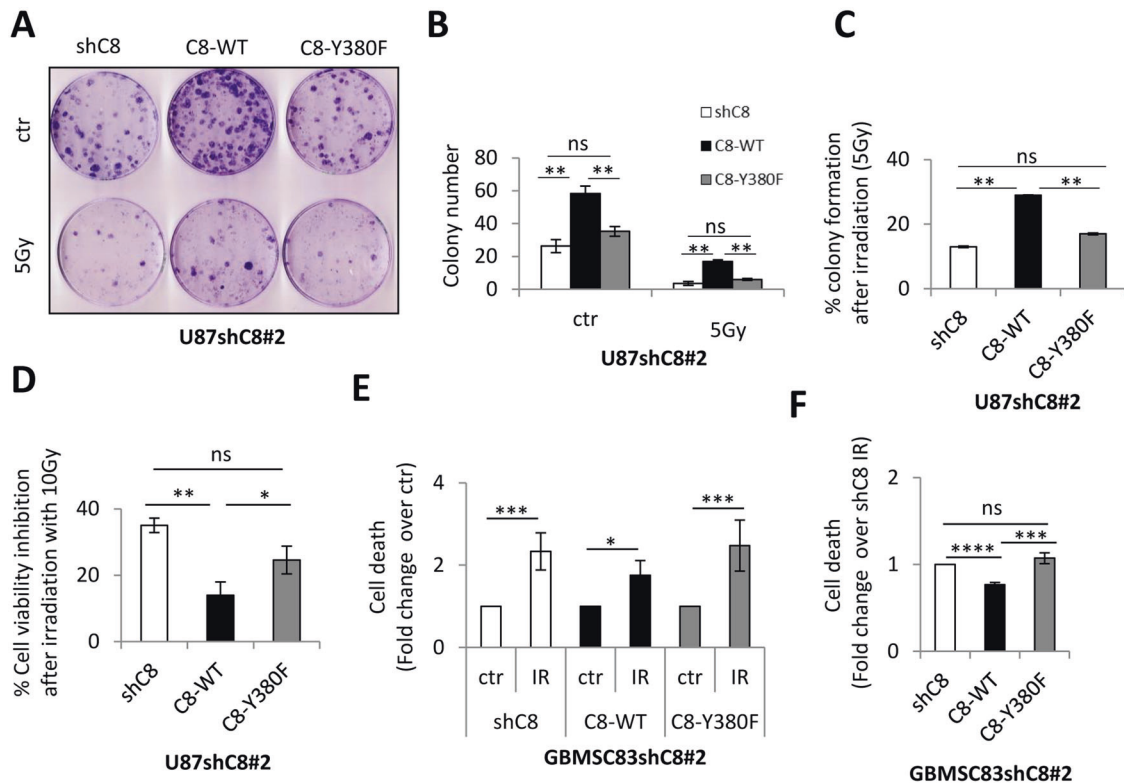


Fig. 6 Src-dependent phosphorylation of Caspase-8 on Y380 promotes glioblastoma cells resistance to ionizing radiation (IR). **A** Representative image of a clonogenic assay performed upon irradiation (IR, 5 Gy) on U87shC8#2 cells stably reconstituted or not with C8-WT or C8-Y380F. **B** Histogram representing colony counts from three independent experiments are presented as mean \pm SE. **C** The histogram shows the percentage of colony formation of U87shC8 cells described in **A** after irradiation, compared to their un-irradiated control. **D** Histogram representing the percentage of cell viability inhibition after IR (10 Gy), evaluated by MTS assay on the same cells used in **A**. **E, F** Histograms representing cell death of GBMSC83shC8#2 and GBMSC83shC8#2 cells stably reconstituted with C8-WT or C8-Y380F, evaluated by flow-cytometry analysis (Annexin V+/PI+ cells) after IR (10 Gy). Statistical analyses were performed by the unpaired Student's *t*-test (ns = not significant; **P* \leq 0.05; ***P* \leq 0.01; ****P* \leq 0.001).

Nevertheless, despite the huge effort to introduce Src-targeting drugs [8] in cancer therapy, the results have been so far disappointing. Interestingly, a novel patient stratification strategy to improve the therapeutic efficacy of Dasatinib in GBM has been recently proposed [37]. Based on a combination of *in silico* and *in vitro* studies the authors suggest that among all GBM tumors, those belonging to the mesenchymal subtype display the higher aberrant activation of Src kinase and consistently are better responders to Dasatinib treatment [37]. This observation, along with the identification in the mesenchymal subtype of higher levels of Caspase-8 and enhanced NF κ B signaling [3] suggest that the Src-Caspase-8-NF κ B axis may indeed represent a molecular signature that identifies tumors that in principle will particularly benefit from Src kinase targeting.

MATERIAL AND METHODS

Cell culture

U87MG (originally obtained by ATCC), U251, and Human Umbilical Vein Cells (HUVEC; PromoCell GmbH, Heidelberg, Germany) were cultured as previously described [10]. GBMSC83 cells, a well-characterized mesenchymal GBM cellular model, were cultured as neurospheres in suspension in DMEM F12 supplied by B27 Supplement (50x), EGF (20 ng/ml), and β FGF (10 ng/ml) as previously described [23, 24]. All GBM cells were routinely tested negative for mycoplasma contamination.

The following sequences were used for stable retroviral Caspase-8 silencing: shC8#1: 5'-ATCACAGACTTTGGACAAA-3'; as control sequence, shCTR: 5'-CTATAACGGCGCTCGATAT-3' [20, 38].

For stable lentiviral Caspase-8 silencing (shC8#2) E42 clone ID TRCN000003579 commercially available (Open Biosystem, Dharmacon, now Horizon) was used according to the manufacture instructions. The original

targeted DNA sequence is 5'-GCCTTGATGTTATCCAGAGA-3'. For the stable reconstitution of Caspase-8-wt and the mutant Caspase-8-Y380F, shC8#2 cell lines were infected with lentiviral pLV-EF1a IRIS vector encoding for Caspase-8-wt or Caspase-8-Y380F carrying the mutations that do alter aminoacidic sequence but confers resistance to the above interference 5'-GCacTtAT GcTtTCCAacGt-3'.

For transient transfection experiments cells were plated the day before and transfected using Lipofectamine2000 (Invitrogen) at 70% of confluence with 1-2 μ g of DNA. Caspase-8 constructs were derived from pcDNA3-Caspase-8-HA (Caspase-8-wt or -Y380F or -C360A or -Y380D or the empty vector, pcDNA3 were used). Src constructs pSGT-Src-Y527F and pSGT-K295R (KD-) were previously described [14].

Antibodies and other reagents

Anti-Caspase-8 (MBL 1:1000, 5F7); anti-pY380-Caspase-8 (EMBL 1:500, E11) anti GAPDH (Santa Cruz 1:5000, D16H11); anti-Vinculin (Cell signaling 1:5000, 13901T), anti-NF- κ B (p65) (Cell signaling 1:1000, 8242S); anti-pSer536-NF- κ B (Cell signaling 1:1000, 3033S); anti-Lamin (Santa Cruz 1:1000, E-1 sc376248), anti-Src (Cell signaling 1:1000, 2108S), anti-pY416-Src (Cell signaling 1:1000, 2101S), anti-IKK α (Santa Cruz 1:200, H-744 sc-7218), anti-IKK β (Santa Cruz 1:200, H-4 sc-8014), anti-I κ B α (Santa Cruz 1:500; H-4 sc-1643); anti-Cleaved Caspase-3 (Cell Signaling 1:500, 5A1E); anti-CD31 (Dianova 1:10, SZ31).

Dasatinib (Sigma Aldrich, DAS) was used 1 μ M or 10 nM for 16 h. Z-VAD-FMK (Sigma Aldrich) was used 10 μ M for 24 h. Cycloheximide (Sigma Aldrich, CHX) was used 10 μ g/ml for 6 h and then, TRAIL (PreProtech) was added 30 ng/ml to the medium for 24 h. Tumor Necrosis Factor alpha (Enzo Life Science, TNF-alpha) was used 10 ng/ml for 30 min.

Immunofluorescence

Cells were plated on coverslips and growth at 37 $^{\circ}$ C and 5% CO $_2$. Before the staining, cells were washed with 1x phosphate buffer saline (PBS) and fixed

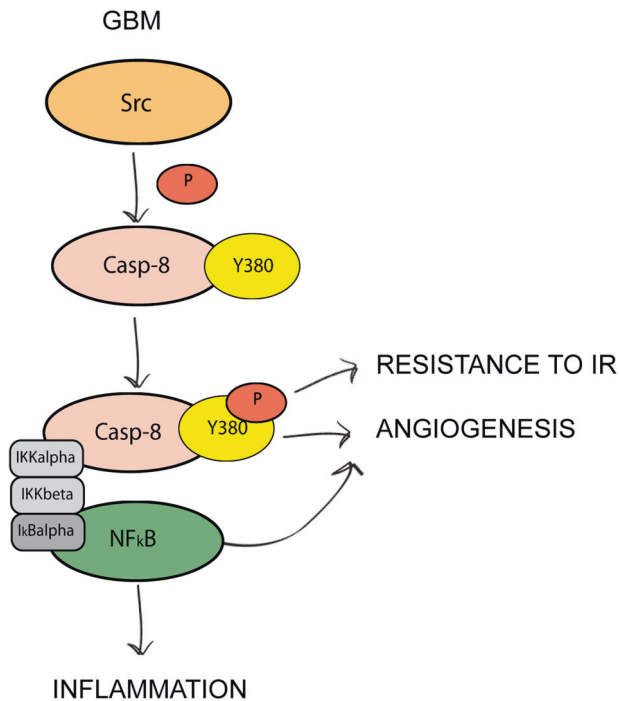


Fig. 7 Schematic illustration of the role of Src-mediated phosphorylation of Caspase-8 on Y380 in glioblastoma. Src non receptor kinase phosphorylates Caspase-8 on Y380 promoting the activation of NF κ B p65 most likely through the formation of a multiprotein complex. Y380 phosphorylation promotes the release of inflammatory and pro-angiogenic factors, the formation of new blood vessels and resistance to ionizing radiation (IR), highlighting a novel role of Src kinase in rewiring Caspase-8 function.

in 4% paraformaldehyde for 20 min at RT, permeabilized in 0.25% Triton x100 for 5 min, blocked with 3% BSA for 1 h at room temperature, and incubated with primary antibody (1:300) overnight in a humid chamber at 4 °C. Secondary antibody (Jackson ImmunoResearch, 1:200) was applied for 1 hr at room temperature, and nuclei were stained with DAPI for 15 min. Confocal microscope (ZEISS LSM 800) was used to obtain pictures of immunostained cells. Cytoplasmic and nuclear staining intensities were analyzed and compared using ImageJ program to obtain the nuclear/cytoplasmic ratio [10].

Protein extracts, immunoprecipitation, nuclei/cytoplasm fractionation and immunoblotting analyses

Total cell extracts, nuclei/cytoplasm cell fractionation, immunoprecipitation and immunoblotting experiments were performed as previously described [10].

Ionizing irradiation and Clonogenic Survival Assay

Control and irradiated (5 Gy) cells were plated in 6-well culture plate (1000 cells/dish) and incubated at 37 °C, 5% CO₂ for colony formation. After 10–15 days, colonies were fixed and stained with a solution with 10% (v/v) methanol and 0.5% Cristal Violet for 20 min for colony visualization. The stained colonies (>50 cells) were counted under a microscope. Data were expressed as mean and SD. The assays were repeated four times.

Cell death analysis

Cell death was evaluated 48 h after ionizing radiation (10 Gy) by using a CytoFLEX S (Beckman Coulter, Milan, Italy) instrument. 1×10^6 cells were collected, centrifuged at 4 °C for 5 min at $300 \times g$ and double-stained by using Annexin V-APC-propidium iodide (PI) kit, according to manufacturer instructions (eBioscience™ Annexin V Apoptosis Detection Kits, ThermoFisher Scientific). Unstained samples were used as control. Quality control was evaluated using CytoFLEX Daily QC Fluorospheres (Beckman

Coulter). FCS files were analyzed using CytExpert version 2.2 software (Beckman Coulter). Dead cells (Annexin V+/PI+ cells) were graphed as fold change to control conditions.

In vitro and in vivo angiogenesis assays

Endothelial capillary tube-like network formation was assessed by plating 2.5×10^4 HUVEC in duplicate in 24-well culture plates containing polymerized Cultrex (Trevigen, Gaithersburg, MD, USA) and incubated with Conditioned Media (CM) from U87shC8 cells, and U87shC8 reconstituted with Caspase-8-wt (C8-WT) or with Caspase-8-Y380F (C8-Y380F) for 6 h. Then, the number of intersection points in ten random microscopic fields were counted.

For in vivo Matrigel assay, 60 μ l 10 \times concentrated CM from the same cells described above, obtained using Centricon-3 concentrators (Merck Millipore, Billerica, MA), were mixed with 600 μ l of Matrigel (BD Bioscience, San Jose, CA), supplemented with heparin (19.2 U; Schwarz Pharma SpA, Milan, Italy). Plugs were injected subcutaneously into the flank of 8-week-old female C57BL/6 mice. Plugs containing heparin alone or heparin plus VEGF (60 ng/mice; R&D Systems, Minneapolis, MN) were used as negative or positive control, respectively. After 5 days, the angiogenic response was evaluated as previously described [10].

Luciferase assay

For reporter gene assay, cells were seeded in a 6-well culture plate and transfected with the indicated amounts of various expression constructs along with pNifty-Luc (Invitrogen) (500 ng) and Renilla (500 ng) using Lipfectamine2000 (Invitrogen). After 24 h, cell extracts were prepared using the Luciferase Cell Culture Lysis Reagent (Promega) and firefly luciferase activity measured using a Victor Multilabel plate reader.

Luminex assay

Concentrations of IL-6, IL-8, MCP-1, IL-1- β and VEGF- α were simultaneously determined in supernatants of U87shC8 cells transiently transfected with pcDNA3, C8-WT or C8-Y380F using a custom-made human magnetic multiplex assay kit (RnD). The assay procedure was performed according to the manufacturer's instructions and the plate was read on a Luminex-200 instrument (Luminex Corp., Austin, TX) and analyzed by XPONENT software. Concentrations of each analyte were calculated using a standard 5P-logistic weighted curve generated for each target and expressed as picograms per milliliter (pg/ml). Due to out of range readings of undiluted samples, analyte concentrations were calculated on 1:10 diluted supernatants.

Reverse transcription and real-time polymerase chain reaction (qPCR)

The Direct-zol RNA Miniprep plus kit (Zymo research) was used for RNA extraction and 500 ng of the extracted RNA was retrotranscribed to a first-strand cDNA, by using SuperScript™ II Reverse Transcriptase enzyme.

qPCR was performed by using the SYBR Green Supermix (SensiFast SYBR Hi-ROX, Bioline) on a StepOne Real-Time PCR System (Applied Biosystems).

The primer pairs used for each gene are listed in supplementary methods.

RNAseq pipeline and statistical analysis

Total RNA was extracted using Qiazol (Qiagen, IT), purified from DNA contamination through a DNase I (Qiagen, IT) digestion step and further enriched by Qiagen RNeasy columns for gene expression profiling (Qiagen, IT). Quantity and integrity of the extracted RNA were assessed by NanoDrop Spectrophotometer (NanoDrop Technologies, DE) and by Agilent 2100 Bioanalyzer (Agilent Technologies, CA), respectively. RNA libraries for sequencing were generated in triplicate using the same amount of RNA for each sample according to the Illumina TruSeq Stranded Total RNA kit with an initial ribosomal depletion step using Ribo Zero Gold (Illumina, CA). The libraries were quantified by qPCR and sequenced in paired-end mode (2×75 bp) with NextSeq 500 (Illumina, CA). For each sample generated by the Illumina platform, a pre-process step for quality control was performed to assess sequence data quality and to discard low-quality reads.

Raw RNA-seq reads were processed via the cloud RNA-seq tool RAP [39] and Differential Expression analysis via Cuffdiff from the Tuxedo Suite [40]. Functional enrichment of significantly regulated genes was performed by using the DAVID functional tool [21] as well as the TRANSFAC database annotation [22]. Fischer exact test was performed to identify the

significantly enriched transcription factors (gene hits, $FDR < 0.05$, R2 correlated genes $FDR < 0.08$). The R2 tool (<http://r2.amc.nl>) was used to identify Caspase-8 significantly ($FDR < 0.05$) correlated (Pearson Correlation > 0.5) genes across the transcriptome data of 540 glioblastoma samples, deposited in the TCGA database. RNA-seq data have been submitted to GEO (GSE193495).

In vivo experiments

Female six weeks old BALB/c nu/nu athymic mice, obtained from Charles River Laboratory, were orthotopically engrafted with GBMSC83 cells (1×10^5 cells in 2.6 μ l) into the right cerebral hemisphere using a Hamilton syringe and a stereotactic micro-injector at a depth of 3.0 mm. Animals were monitored until onset of neurological sequelae, including hunched posture and weight loss, at which point they were sacrificed. Brain samples were fixed with 4% formaldehyde, sliced into sections followed by staining with hematoxylin-eosin and CD31 antibody. Animal experiments were approved by the UCSD Animal Care Program, protocol number S00192M, and were performed under IACUC regulations.

Statistical analyses

All experiments were replicated at least three times (biological replicates) and data were presented as mean \pm SD or \pm SE, as indicated in the figure legends. Sample sizes were chosen based on preliminary results to ensure a power of 80% and an alpha level of 5%. No data or animals were excluded from the analyses. The significance of the differences between populations of data were assessed according to the Student's two-tailed *t*-test or The Mann-Whitney test (independent samples) with level of significance of at least $P \leq 0.05$.

DATA AVAILABILITY

All data needed to evaluate the conclusions in the paper are present in the paper and/or the Supplementary Materials. Additional data related to this paper may be requested from the authors.

REFERENCES

- Network CGAR. Comprehensive genomic characterization defines human glioblastoma genes and core pathways. *Nature*. 2008;455:1061–8.
- Stupp R, Mason WP, van den Bent MJ, Weller M, Fisher B, Taphoorn MJ, et al. Radiotherapy plus concomitant and adjuvant temozolomide for glioblastoma. *N Engl J Med*. 2005;352:987–96.
- Verhaak RG, Hoadley KA, Purdom E, Wang V, Qi Y, Wilkerson MD, et al. Integrated genomic analysis identifies clinically relevant subtypes of glioblastoma characterized by abnormalities in PDGFRA, IDH1, EGFR, and NF1. *Cancer Cell*. 2010;17:98–110.
- Brennan CW, Verhaak RG, McKenna A, Campos B, Nourbakhsh H, Salama SR, et al. The somatic genomic landscape of glioblastoma. *Cell*. 2013;155:462–77.
- Bjorge JD, Jakymiw A, Fujita DJ. Selected glimpses into the activation and function of Src kinase. *Oncogene*. 2000;19:5620–35.
- Ahluwalia MS, de Groot J, Liu WM, Gladson CL. Targeting SRC in glioblastoma tumors and brain metastases: rationale and preclinical studies. *Cancer Lett*. 2010;298:139–49.
- Du J, Bernasconi P, Clauser KR, Mani DR, Finn SP, Beroukhi R, et al. Bead-based profiling of tyrosine kinase phosphorylation identifies SRC as a potential target for glioblastoma therapy. *Nat Biotechnol*. 2009;27:77–83.
- Cirotti C, Contadini C, Barilà D. SRC kinase in glioblastoma: news from an old acquaintance. *Cancers*. 2020;12:1558.
- Stupack DG. Caspase-8 as a therapeutic target in cancer. *Cancer Lett*. 2013;332:133–40.
- Fianco G, Mongiardi MP, Levi A, De Luca T, Desideri M, Triscioglio D, et al. Caspase-8 contributes to angiogenesis and chemotherapy resistance in glioblastoma. *Elife*. 2017;6:e22593.
- Müller I, Strozzyk E, Schindler S, Beissert S, Oo HZ, Sauter T, et al. Cancer cells employ nuclear Caspase-8 to overcome the p53-dependent G2/M checkpoint through cleavage of USP28. *Mol Cell*. 2020;77:970–84. e977.
- Fianco G, Contadini C, Ferri A, Cirotti C, Stagni V, Barilà D. Caspase-8: a novel target to overcome resistance to chemotherapy in glioblastoma. *Int J Mol Sci*. 2018;19:3798.
- Fulda S. Cell death-based treatment of glioblastoma. *Cell Death Dis*. 2018;9:121.
- Cursi S, Rufini A, Stagni V, Condo I, Matafora V, Bachi A, et al. Src kinase phosphorylates caspase-8 on Tyr380: a novel mechanism of apoptosis suppression. *Embo J*. 2006;25:1895–905.
- Powley IR, Hughes MA, Cain K, MacFarlane M. Caspase-8 tyrosine-380 phosphorylation inhibits CD95 DISC function by preventing procaspase-8 maturation and cycling within the complex. *Oncogene*. 2016;35:5629–40.
- Torres VA, Mielgo A, Barila D, Anderson DH, Stupack D. Caspase 8 promotes peripheral localization and activation of Rab5. *J Biol Chem*. 2008;283:36280–9.
- Barbero S, Barila D, Mielgo A, Stagni V, Clair K, Stupack D. Identification of a critical tyrosine residue in caspase 8 that promotes cell migration. *J Biol Chem*. 2008;283:13031–4.
- Barbero S, Mielgo A, Torres V, Teitz T, Shields DJ, Mikolon D, et al. Caspase-8 association with the focal adhesion complex promotes tumor cell migration and metastasis. *Cancer Res*. 2009;69:3755–63.
- Keller N, Ozmadenci D, Ichim G, Stupack D. Caspase-8 function, and phosphorylation, in cell migration. *Semin Cell Dev Biol*. 2018;82:105–17.
- Fianco G, Cenci C, Barilà D. Caspase-8 expression and its Src-dependent phosphorylation on Tyr380 promote cancer cell neoplastic transformation and resistance to anoikis. *Exp Cell Res*. 2016;347:114–22.
- Huang DW, Sherman BT, Lempicki RA. Systematic and integrative analysis of large gene lists using DAVID bioinformatics resources. *Nat Protoc*. 2009;4:44–57.
- Wingender E, Dietze P, Karas H, Knüppel R. TRANSFAC: a database on transcription factors and their DNA binding sites. *Nucleic Acids Res*. 1996;24:238–41.
- Minata M, Audia A, Shi J, Lu S, Bernstock J, Pavlyukov MS, et al. Phenotypic plasticity of invasive edge glioma stem-like cells in response to ionizing radiation. *Cell Rep*. 2019;26:1893–905. e1897.
- Mao P, Joshi K, Li J, Kim SH, Li P, Santana-Santos L, et al. Mesenchymal glioma stem cells are maintained by activated glycolytic metabolism involving aldehyde dehydrogenase 1A3. *Proc Natl Acad Sci USA*. 2013;110:8644–9.
- Humphreys L, Espona-Fiedler M, Longley DB. FLIP as a therapeutic target in cancer. *FEBS J*. 2018;285:4104–23.
- Oztürk S, Schleich K, Lavrik IN. Cellular FLICE-like inhibitory proteins (c-FLIPs): finetuners of life and death decisions. *Exp Cell Res*. 2012;318:1324–31.
- Henry CM, Martin SJ. Caspase-8 acts in a non-enzymatic role as a scaffold for assembly of a pro-inflammatory “FADDosome” complex upon TRAIL stimulation. *Mol Cell*. 2017;65:715–29. e715.
- Chaudhary PM, Eby MT, Jasmin A, Kumar A, Liu L, Hood L. Activation of the NF-kappaB pathway by caspase 8 and its homologs. *Oncogene*. 2000;19:4451–60.
- Su H, Bidère N, Zheng L, Cubre A, Sakai K, Dale J, et al. Requirement for caspase-8 in NF-kappaB activation by antigen receptor. *Science*. 2005;307:1465–8.
- Bidère N, Snow AL, Sakai K, Zheng L, Lenardo MJ. Caspase-8 regulation by direct interaction with TRAF6 in T cell receptor-induced NF-kappaB activation. *Curr Biol*. 2006;16:1666–71.
- Rébé C, Cathelin S, Launay S, Filomenko R, Prévotat L, L'Ollivier C, et al. Caspase-8 prevents sustained activation of NF-kappaB in monocytes undergoing macrophagic differentiation. *Blood*. 2007;109:1442–50.
- Moen SH, Westhlin M, Zahoor M, Nørgaard NN, Hella H, Størdal B, et al. Caspase-8 regulates the expression of pro- and anti-inflammatory cytokines in human bone marrow-derived mesenchymal stromal cells. *Immun Inflamm Dis*. 2016;4:327–37.
- Keller N, Mares J, Zerbe O, Grütter MG. Structural and biochemical studies on procaspase-8: new insights on initiator caspase activation. *Structure*. 2009;17:438–48.
- Keller N, Grütter MG, Zerbe O. Studies of the molecular mechanism of caspase-8 activation by solution NMR. *Cell Death Differ*. 2010;17:710–8.
- Bhat KPL, Balasubramanian V, Vaillant B, Ezhilarasan R, Hummelink K, Hollingsworth F, et al. Mesenchymal differentiation mediated by NF- κ B promotes radiation resistance in glioblastoma. *Cancer Cell*. 2013;24:331–46.
- Pordanjani SM, Hosseinimehr SJ. The Role of NF- κ B inhibitors in cell response to radiation. *Curr Med Chem*. 2016;23:3951–63.
- Alhalabi OT, Fletcher MNC, Hielscher T, Kessler T, Lokumcu T, Baumgartner U, et al. A novel patient stratification strategy to enhance the therapeutic efficacy of dasatinib in glioblastoma. *Neuro Oncol*. 2021;24:39–51.
- Stagni V, Mingardi M, Santini S, Giaccari D, Barila D. ATM kinase activity modulates cFLIP protein levels: potential interplay between DNA damage signalling and TRAIL-induced apoptosis. *Carcinogenesis*. 2010;31:1956–63.
- D'Antonio M, D'Onorio De Meo P, Pallocca M, Picardi E, D'Erchia AM, Calogero RA, et al. RAP: RNA-Seq Analysis Pipeline, a new cloud-based NGS web application. *BMC Genomics*. 2015;16:53.
- Trapnell C, Roberts A, Goff L, Pertea G, Kim D, Kelley DR, et al. Differential gene and transcript expression analysis of RNA-seq experiments with TopHat and Cufflinks. *Nat Protoc*. 2012;7:562–78.

ACKNOWLEDGEMENTS

We thank Maria Pia Gentileschi for kindly providing technical support for irradiation experiments and all the members of our lab for critical reading of the manuscript and for helpful discussion.

AUTHOR CONTRIBUTIONS

CCo performed most of the experiments, data analysis, interpretation and contributed to write the article; AF performed experiments with ionizing radiation; MDM performed angiogenesis studies; CCI performed cell death analysis experiments and qRT-PCR experiments; DDB designed angiogenesis studies; FDN performed the RNAseq experiments; MP, MF, FS performed bioinformatic analyses; GD and AC performed Luminex experiments; EV designed Luminex experiments; NK generated Caspase-8 lentiviral constructs; SM, DK conducted in vivo experiments; DS contributed to write the manuscript and to analyze the data; FF contributed to in vivo experimental design, data analysis and manuscript editing; DB designed the experiments, evaluated the data and wrote the paper.

FUNDING

This work has been supported by research grants from Associazione Italiana per la Ricerca sul Cancro AIRC-IG2016-n.19069, AIRC-IG2021-n.26230, and Italian Ministry of Health, RF-2016-02362022 to DB; CCo work also been supported by AIRC-IG2016-n.19069 and AIRC-IG2021-n.26230, AF PhD fellowship was supported from MUR; MDM was supported by a FIRC-AIRC fellowship for Italy. The research leading to these results has received funding from AIRC under IG 2020 - ID. 24315 project - P.I. DDB; CCI has been supported by a FIRC-AIRC fellowship for Italy "Filomena Todini". This work was also supported by United States National Institutes of Health (NIH) grants NS080939, NS116802, and CA258248 (FF).

COMPETING INTERESTS

The authors declare no competing interests.

ETHICS APPROVAL

All procedures involving mice handling and care conformed to protocols approved by the Regina Elena National Cancer Institute (Rome, Italy) in compliance with national (D.L. N.116, G.U., suppl. 40, 18-2-1992 and N. 26, G.U. March 4, 2014) and international (EEC Council Directive 2010/63/EU, OJ L 276/33, 22-09-2010; National Institutes of Health Guide for the Care and Use of Laboratory Animals, US National Research Council, 2011) law and policies. The study was approved by the Italian Ministry of Health (approval number:342/2019-PR).

ADDITIONAL INFORMATION

Supplementary information The online version contains supplementary material available at <https://doi.org/10.1038/s41418-022-01093-x>.

Correspondence and requests for materials should be addressed to Daniela Barilà.

Reprints and permission information is available at <http://www.nature.com/reprints>

Publisher's note Springer Nature remains neutral with regard to jurisdictional claims in published maps and institutional affiliations.

Springer Nature or its licensor (e.g. a society or other partner) holds exclusive rights to this article under a publishing agreement with the author(s) or other rightsholder(s); author self-archiving of the accepted manuscript version of this article is solely governed by the terms of such publishing agreement and applicable law.